

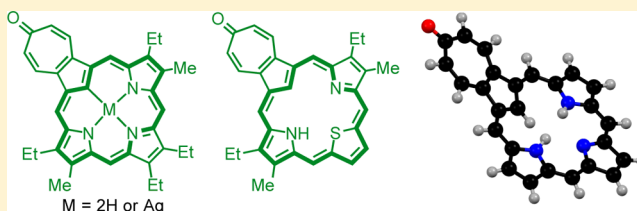
Tropone-Fused Carbaporphyrins

Timothy D. Lash,* Gean C. Gilot, and Deyaa I. AbuSalim

Department of Chemistry, Illinois State University, Normal, Illinois 61790-4160, United States

S Supporting Information

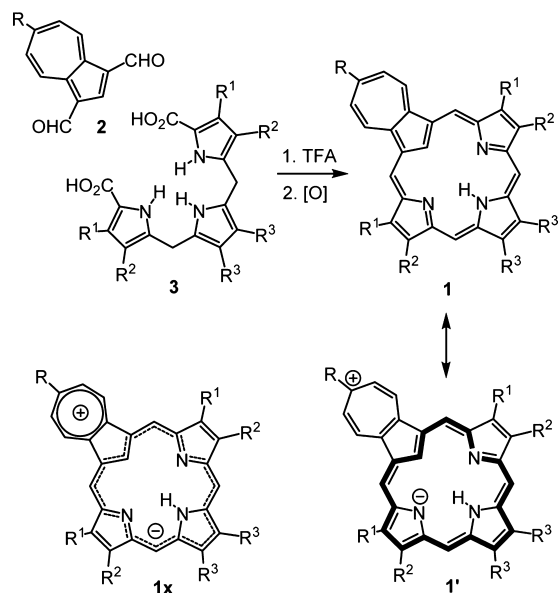
ABSTRACT: Previous attempts to prepare tropone-fused carbaporphyrins by reacting peroxides with azuliporphyrins under basic conditions afforded benzocarbaporphyrins instead. In this study, a methoxyazulitripyrrane condensed with a pyrrole dialdehyde in the presence of TFA, followed by oxidation with ferric chloride, to give a tropone-fused carbaporphyrin following a spontaneous demethylation. The porphyrinoid gave a modified UV–vis spectrum showing multiple bands in the Soret region, and the proton NMR spectrum showed that it has a reduced diamagnetic ring current in comparison to other carbaporphyrins. The tropone-fused derivative failed to react with *tert*-butyl hydroperoxide and potassium hydroxide, demonstrating that this type of structure is not an intermediate in the formation of benzocarbaporphyrins. However, the reaction with silver(I) acetate gave the corresponding silver(III) complex. Condensation of the methoxyazulitripyrrane with 2,5-thiophenedicarbaldehyde gave a related tropone-fused thiocarbaporphyrin together with a methoxythiaazuliporphyrin. Treatment of the carbaporphyrins with DBU resulted in the formation of anionic species, while addition of acid afforded dicationic structures. DFT studies were performed on a series of tautomers, protonated species, and anionic structures related to these tropone-fused carbaporphyrins, and NICS calculations were carried out. These results allowed favorable conjugation pathways to be identified. In addition, these studies predicted that protonation initially occurs on the carbonyl moiety rather than on the expected interior pyrroline nitrogen atom.



INTRODUCTION

Azuliporphyrins (e.g., **1**) are porphyrin analogues with an azulene unit in place of a pyrrole moiety.^{1,2} The first synthesis of this system was carried out by reacting 1,3-azulenedicarbaldehyde (**2**) with the tripyrrane **3** in the presence of trifluoroacetic acid, followed by oxidation with DDQ (Scheme 1).¹ Azuliporphyrins are cross-conjugated but retain significant diatropic character that has been attributed to dipolar resonance contributors such as **1'** that retain 18- π -electron delocalization pathways.^{1,2} However, an analysis of the bond lengths determined by X-ray diffraction analyses for an azuliporphyrin³ and two related heteroazuliporphyrins⁴ indicated that the favored delocalization pathway involves the presence of a 17-atom circuit, as illustrated in structure **1x**. The diatropic character of azuliporphyrins is modest in comparison to that of porphyrins and carbaporphyrins,⁵ but the internal CH is shifted upfield to approximately 3 ppm.³ Similar observations have also been made for *meso*-tetraarylazuliporphyrins⁶ and benzoazuliporphyrins.⁷ The favorability of zwitterionic canonical forms for **1** leads to these compounds being relatively polar, and the tropylium character for the seven-membered ring makes this system susceptible to nucleophilic attack.⁸ For instance, azuliporphyrins form adducts **4** in the presence of pyrrolidine that take on fully aromatic carbaporphyrin-like characteristics (Scheme 2).^{6,8} Although this type of addition product is generated in equilibrium with the free base azuliporphyrin, these species can easily be characterized by NMR spectroscopy.^{2,6,8} It was speculated that this reactivity could be harnessed to generate carbaporphyrins with fused

Scheme 1

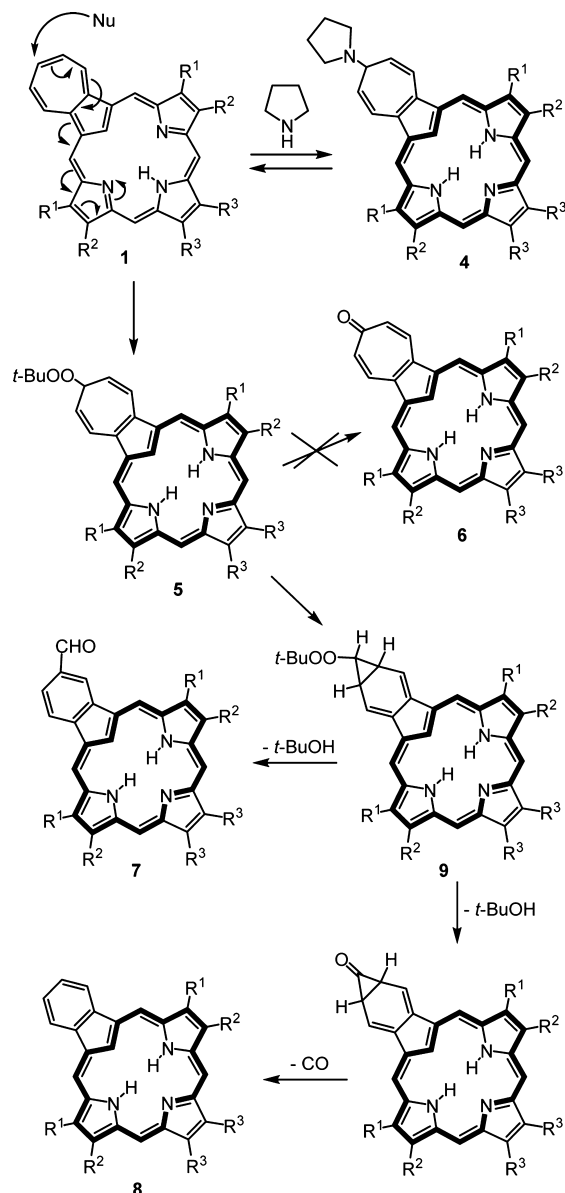


tropone units that could potentially exhibit unique characteristics (Scheme 2).⁸ With this in mind, azuliporphyrin **1** was reacted with *tert*-butyl hydroperoxide in the presence of base. It

Received: August 11, 2014

Published: September 17, 2014

Scheme 2



was anticipated that initial nucleophilic attack by the *tert*-butyl hydroperoxide anion would give the peroxide adduct 5 and subsequent elimination of *tert*-butyl alcohol would then afford the troponone-fused carbaporphyrin 6.⁸ However, no trace of 6 could be detected and benzocarporphyrins 7 and 8 were generated instead (Scheme 2).⁸ Although it is conceivable that 6 was an intermediate in the generation of the observed products, an alternative mechanism was proposed for their formation (Scheme 2).⁸ A Cope rearrangement of 5 could produce the norcaradiene-fused carbaporphyrin 9, and subsequent loss of *tert*-BuOH would then afford the observed aldehyde 7 or a cyclopropanone derivative. Extrusion of carbon monoxide from the latter species would yield benzocarporphyrin 8. An additional carbaporphyrin monoaldehyde product is observed in these reactions, arising from nucleophilic attack at a different position on the seven-membered ring.^{2,6,8}

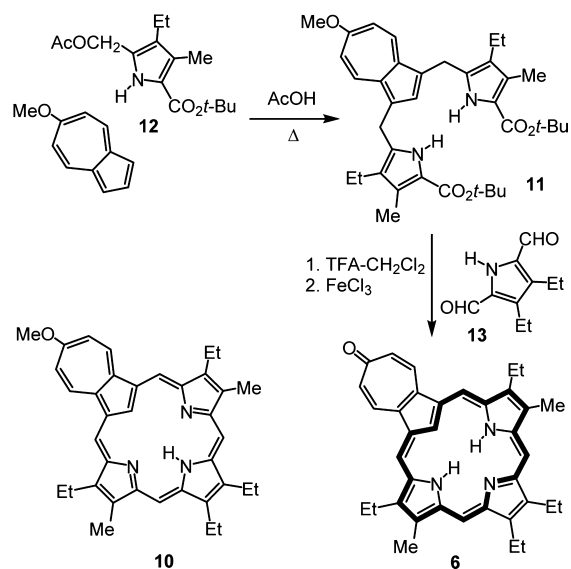
Azuliporphyrins have been shown to readily form nickel(II),⁹ palladium(II),⁹ platinum(II),⁹ iridium(II),¹⁰ and ruthenium¹¹ organometallic derivatives and are selectively oxidized on the internal carbon in the presence of copper(II) salts.¹² Given the

interesting properties of azuliporphyrins, the influence of substituents attached to the azulene subunit was explored, and it was noted that the presence of a *tert*-butyl moiety slightly enhanced the diatropic characteristics of the system.^{3,13} This effect was attributed to the electron-donating *tert*-butyl group stabilizing the tropylium character of contributors such as 1' and 1x that possess 18- π -electron delocalization pathways. In an attempt to further probe this phenomenon, azuliporphyrins with a more strongly electron donating methoxy substituent were targeted for synthesis. However, these studies instead resulted in the formation of the formerly elusive troponone-fused carbaporphyrins 6. The synthesis and characterization of these novel derivatives are presented, and the formation of a silver(III) complex is reported.¹⁴

RESULTS AND DISCUSSION

Although the original synthetic route to azuliporphyrins involved the reaction of an azulene dialdehyde with the tripyrrolic species 3 (Scheme 1),¹ an alternative “3 + 1” approach was developed where an azulene-containing tripyrrene analogue was used as the key intermediate.¹⁵ Using this methodology, the synthesis of methoxyazuliporphyrin 10 would necessitate the intermediacy of azulitripyrrene 11 (Scheme 3).

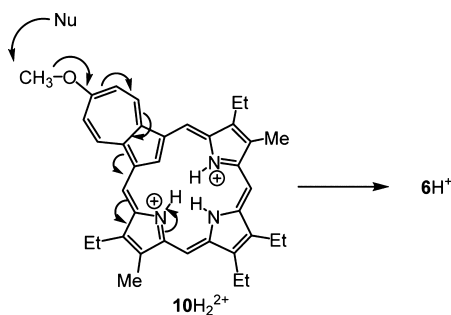
Scheme 3



6-Methoxyazulene¹⁶ was reacted with 2 equiv of acetoxymethylpyrrole 12 in refluxing acetic acid–ethanol, and following purification by column chromatography on silica and recrystallization from hexanes, azulitripyrrene 11 was isolated in 72% yield (Scheme 3). The tripyrrene analogue was treated with trifluoroacetic acid for 10 min to cleave the *tert*-butyl ester protective groups and then diluted with dichloromethane and reacted with pyrrole dialdehyde 13.^{17,18} Following oxidation with aqueous ferric chloride solution, the crude product was purified by column chromatography. A brown fraction corresponding to a mixture of benzocarporphyrins eluted initially, followed by a major fraction corresponding to the porphyrinoid product. However, the isolated product was not the expected methoxyazuliporphyrin 10 but instead turned out to be the troponone-fused carbaporphyrin 6. Following recrystallization, the carbaporphyrin was isolated as purple crystals in 32% yield. A polar green fraction also eluted from the

column but could not be identified. The possibility of forming **6** from protonated methoxyazuliporphyrin 10H_2^{2+} had been anticipated as $\text{S}_{\text{N}}2$ attack onto the methoxy unit that would displace the tropone-fused porphyrinoid as a favorable leaving group (Scheme 4). Clearly demethylation occurs very easily under the mild reaction conditions utilized in the “3 + 1” synthesis.

Scheme 4



The UV–vis spectrum for **6** differed significantly from the spectra for carbaporphyrins such as **7** and **8**. Benzocarbaporphyrin **8** gives a strong Soret band at 424 nm and weaker Q bands at 510, 544, 602, and 662 nm.^{5a} In contrast, **6** does not afford a Soret-type band but instead gives several medium-sized peaks in the 350–500 nm range (Figure 1) that are similar to

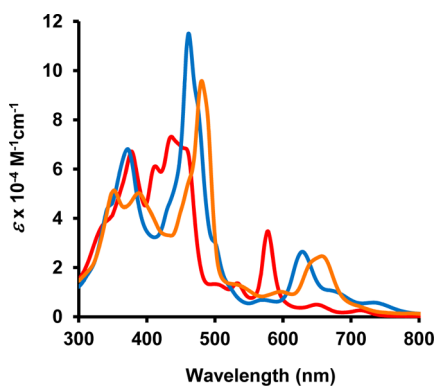
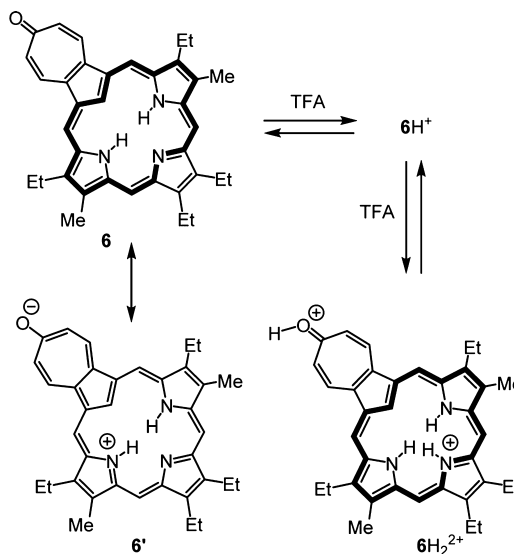


Figure 1. UV–vis spectra of tropone-fused carbaporphyrin **6**: free base in 1% $\text{Et}_3\text{N}-\text{CH}_2\text{Cl}_2$ (red line); dication 6H_2^{2+} in 1% $\text{TFA}-\text{CH}_2\text{Cl}_2$ (blue line); anion $[6\text{-H}]^-$ in 5% $\text{DBU}-\text{CH}_2\text{Cl}_2$ (orange line).

peaks in this region in the spectra for azuliporphyrins.^{2,19} However, the longer wavelength region gave rise to Q bands at 533, 578, 650, and 715 nm that more closely resemble the spectra for porphyrins and carbaporphyrins, although the peak at 578 nm is relatively intense (Figure 1). Azuliporphyrins only give broad bands in this region; therefore, the spectrum for **6** represents a hybrid of these very different porphyrin analogue systems. This result implies that there is a strong electronic interaction between the carbaporphyrin core and the fused tropone unit that can be represented with resonance contributors such as **6'**. This supposition is supported by the IR spectrum of **6**, which showed the carbonyl stretching frequency at a relatively low value of 1596 cm^{-1} . This is in contrast with a value of 1638 cm^{-1} that has been reported for tropone itself.²⁰ Addition of trace amounts of TFA to a solution of **6** in dichloromethane showed the formation of an intermediary species that was assigned as the monocation

6H^+ , but further addition of acid led to a new chromophore that was attributed to the dication 6H_2^{2+} (Scheme 5). The UV–vis spectrum of 6H_2^{2+} in 1% TFA–dichloromethane is far more porphyrin-like, showing Soret bands at 372 and 461 nm and Q-type bands at longer wavelengths (Figure 1).

Scheme 5



The proton NMR spectrum for **6** in CDCl_3 showed that the system retains highly diatropic characteristics and the internal CH gave a resonance upfield at -7.64 ppm , while the NH protons gave rise to a broad peak at -4.47 ppm (Figure 2).

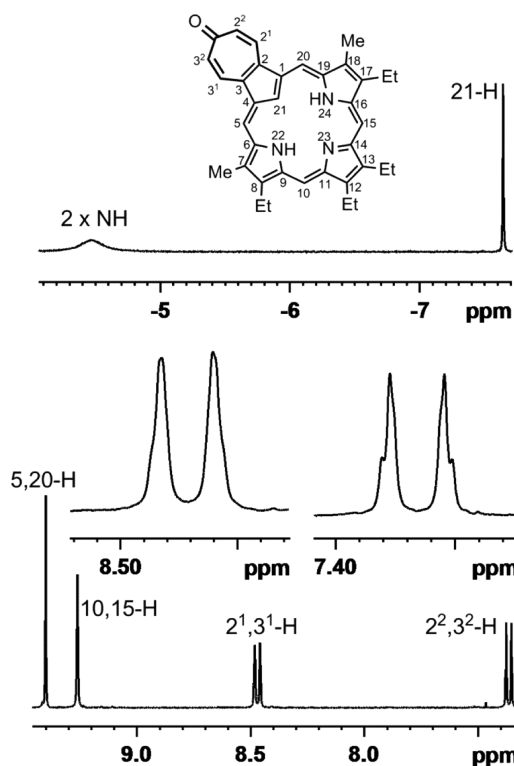


Figure 2. Partial 500 MHz proton NMR spectrum for the tropone-fused carbaporphyrin **6** in CDCl_3 at 300 K showing the upfield and downfield regions.

However, the external *meso* protons were not as far downfield as is seen for porphyrins and carbaporphyrins such as **8**,^{21–23} which typically give values of 10 ppm, and showed up as two 2H singlets at 9.26 and 9.40 ppm. The slightly reduced deshielding effect can be attributed to contributions by the cross-conjugated canonical form **6'**. The tropone unit gave rise to two 2H doublets at 7.41 and 8.45 ppm that are consistent with the presence of conjugated enone units which do not contribute to the aromatic delocalization pathway. The presence of a plane of symmetry is evident in both the proton and carbon-13 NMR spectra. In the carbon-13 NMR spectrum, the *meso* carbons were identified at 95.1 and 100.0 ppm, while the internal carbon (C-21) appeared at 102.6 ppm. The presence of a carbonyl group was confirmed by the presence of a resonance at 188.1 ppm. The proton NMR spectrum of **6H₂²⁺** in TFA–CHCl₃ also shows the presence of a strong diamagnetic ring current (Figure 3). Although the internal

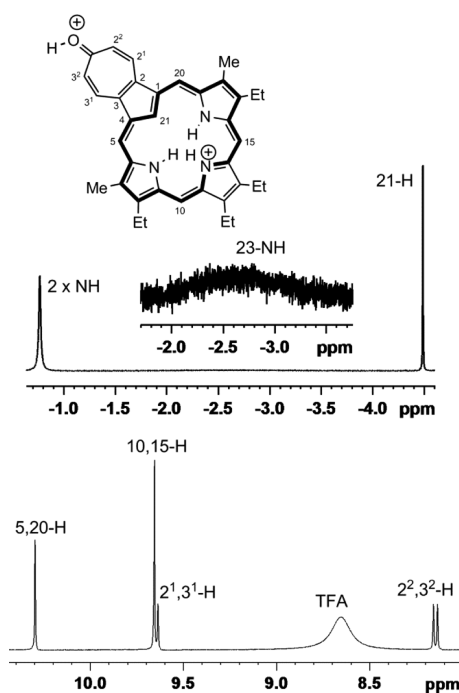
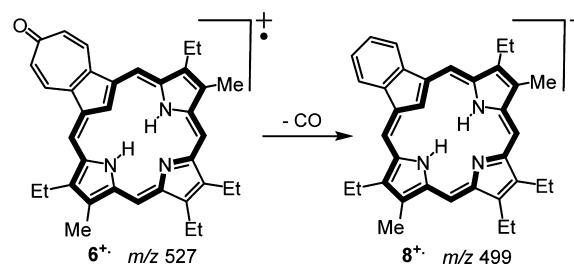


Figure 3. Partial 500 MHz proton NMR spectrum of dication **6H₂²⁺** in TFA–CDCl₃ showing the upfield and downfield regions.

protons are not shifted as far upfield (the CH appears at –4.40 ppm, while the NHs give rise to broad peaks at –2.60 (1H) and –0.68 (2H) ppm), the *meso* protons gave downfield resonances at 9.74 and 10.38 ppm. In addition, the tropone protons were also shifted downfield, giving rise to two 2H doublets at 8.23 and 9.73 ppm. These differences can primarily be attributed to the positive charges associated with this species. The carbon-13 NMR spectrum again showed that the porphyrin analogue retains a plane of symmetry and the *meso* carbons now appeared at 95.5 and 109.1 ppm, while the internal carbon gave a resonance at 118.9 ppm. The structure of **6** was also confirmed by high-resolution mass spectrometry. Interestingly, in the electron impact mass spectrum for **6** the base peak was *m/z* 499. This corresponds to a fragment that had extruded CO (confirmed by HR MS: calculated for C₃₅H₃₇N₃ 499.2987, found 499.2993) to give the benzocarbaporphyrin radical cation **8[•]** (Scheme 6). Unfortunately, the tropone-fused porphyrin failed to lose CO even when it was heated under vacuum for 16

Scheme 6

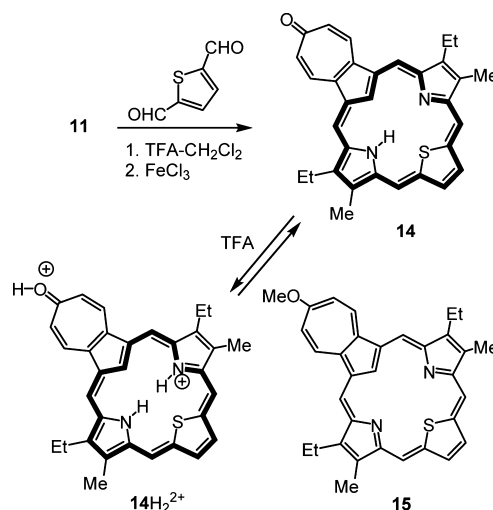


h at 200 °C; therefore, this observation does not appear to provide a viable route to benzocarbaporphyrins.

During studies into the oxidative ring contraction of azuliporphyrins (Scheme 2), the tropone-fused carbaporphyrin **6** could not be excluded as a possible intermediate in the formation of benzocarbaporphyrins. In order to obtain further information about this reaction, **6** was treated with *t*-BuOOH and KOH in CH₂Cl₂–MeOH under the conditions originally used in reactions with azuliporphyrins. Even after a period of several hours, no reaction was observed. Therefore, it can be safely concluded that **6** cannot be an intermediate in this chemistry.

In order to further explore the “3 + 1” synthesis, azulitripyrrane **11** was reacted with 2,5-thiophenedicarbaldehyde under the same conditions. In this case, two major products were observed, in addition to a minor fraction corresponding to impure benzothiacarbaporphyrins. The less polar fraction corresponded to tropone-fused carbaporphyrin **14**, but a polar green fraction could also be isolated corresponding to the methoxythiaazuliporphyrin **15** (Scheme 7). Although the combined yields of the two porphyrinoids

Scheme 7



were fairly consistent (ca. 40%), the ratio of the two differed somewhat from one experiment to the next. Thiocarbaporphyrin **14** was poorly soluble in organic solvents, but proton NMR data could be obtained in CDCl₃ and a low-quality carbon-13 NMR spectrum was obtained at 50 °C. The proton NMR spectrum for **14** at 50 °C showed the inner CH at –6.79 ppm and a very broad peak at –4.7 ppm for the NH. The *meso* protons gave two downfield 2H singlets at 9.17 and 9.89 ppm, while the thiophene protons appeared as a 2H singlet at 9.56

ppm. The results are consistent with an aromatic system exhibiting diatropic character similar to that of carbaporphyrin **6**. The proton and carbon-13 NMR spectra for **14** were consistent with a species that has a plane of symmetry, and this indicates that the NH proton must be undergoing rapid exchange. The IR spectrum again showed a low-frequency value for carbonyl stretching (1591 cm^{-1}), but the carbonyl unit could be identified as a resonance at 187.9 ppm in the carbon-13 NMR spectrum. The UV-vis spectrum of **14** in dichloromethane gave two broadened peaks in the Soret region and several Q bands at higher wavelengths (Figure 4).

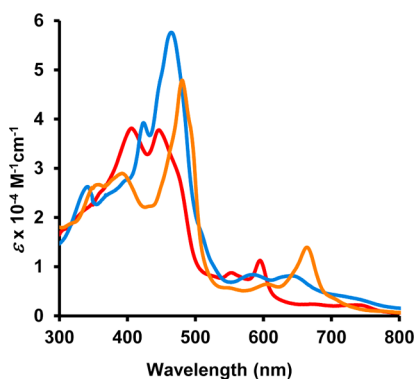
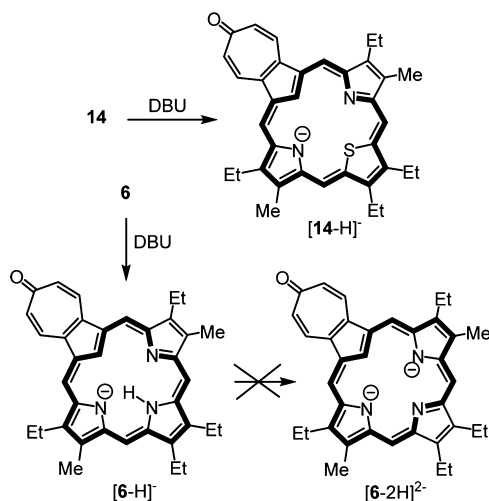


Figure 4. UV-vis spectra of tropone-fused thiacarporphyrin **14**: free base in CH_2Cl_2 (red line); dication 14H_2^{2+} in 1% TFA- CH_2Cl_2 (blue line); anion $[14\text{-H}]^-$ in 1% DBU- CH_2Cl_2 (orange line).

Again, this spectrum appeared to be similar to that of an azuliporphyrin in the 400–500 nm region but more closely resembled that of a carbaporphyrin between 550 and 800 nm. In our studies, we often run the UV-vis spectra of free base porphyrinoids in the presence of 1% triethylamine in order to ensure that protonation due to acid contamination from the chlorinated solvent does not occur. However, in this case the spectrum was slightly altered due to partial deprotonation of the system. In the presence of 1% DBU, the spectrum for the new species $[14\text{-H}]^-$ (Scheme 8) was obtained that showed a Soret band at 480 nm and several weaker bands at longer wavelengths (Figure 4). A proton NMR spectrum of **14** in the presence of DBU showed the *meso* and thiophene protons

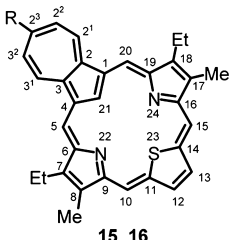
Scheme 8



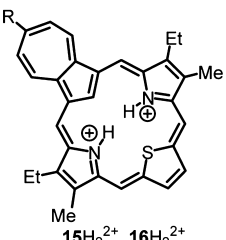
downfield as three 2H singlets between 9.4 and 9.9 ppm, while the internal CH gave a broad upfield singlet at -3.08 ppm . These results demonstrate that the anionic species retains highly diatropic characteristics. The UV-vis spectrum of tropone-fused carbaporphyrin **6** was also examined in the presence of DBU, and this too afforded a new chromophore that was attributed to the anionic species $[6\text{-H}]^-$. However, further addition of DBU failed to generate the corresponding dianion $[6\text{-2H}]^{2-}$. The UV-vis spectrum of the monoanion gave a Soret band at 480 nm and a moderately strong absorption at 664 nm (Figure 1). The proton NMR spectrum of **6** in the presence of DBU again showed that the anion retains a strong diatropic ring current and the internal CH appeared at -6.45 ppm . Addition of trace amounts of TFA to solutions of **14** showed the initial formation of a monocationic species by UV-vis spectroscopy, but further protonation to give the dication 14H_2^{2+} occurred readily (Scheme 7). The UV-vis spectrum of the dication in 1% TFA-dichloromethane showed a broad Soret band at 465 nm and broadened Q bands at higher wavelengths (Figure 4). The proton NMR spectrum of 14H_2^{2+} in TFA- CDCl_3 showed the *meso* protons as two downfield singlets at 10.76 and 10.77 ppm and the thiophene protons at 10.10 ppm, while the interior CH gave an upfield singlet at -4.73 ppm and the NH protons appeared as a broad peak at -2.51 ppm . These results show that the system remains highly diatropic, and the proton and carbon-13 NMR spectra also confirm that the macrocycle retains a plane of symmetry.

6-Methoxythiazuliporphyrin **15** was poorly soluble in organic solvents, but a proton NMR spectrum of the free base could be obtained in CDCl_3 . This spectrum showed a degree of aromatic character, but the anticipated enhanced diamagnetic ring current due to the presence of a methoxy substituent was not observed (Table 1). The *meso* protons were observed near 9 ppm, while a broad peak for the internal CH was seen at 2.93. The upfield and downfield shifts for the inner and outer protons, respectively, are actually slightly reduced in comparison to the signals for thiazuliporphyrin **16a** or the related *tert*-butylthiazuliporphyrin **16b**. In the presence of trifluoroacetic acid, the dication 15H_2^{2+} was generated (Scheme 7) and, as expected, this species showed greatly increased diatropic character (Table 1). The *meso* protons were observed as two 2H singlets at 10.83 and 10.72 ppm, while the inner 21-H appeared upfield at -4.24 ppm . As the protons at positions 10 and 15, 12 and 13, and 21 are furthest removed from the methoxy group, these resonances give the best measure of overall macrocyclic diatropicity. There is an indication that the diatropic character is slightly increased in 15H_2^{2+} in comparison to $16a\text{H}_2^{2+}$ or $16b\text{H}_2^{2+}$, which could be attributed to contributions from the canonical form $15'\text{H}_2^{2+}$ (Scheme 9), but the effect is very small. It is worth noting that the presence of a *tert*-butyl group can stabilize tropylium character in structures such as **1'** and **1x**, but a methoxy unit would actually inductively destabilize this type of resonance structure. Presumably, the electron-donating effect of the methoxy group is not sufficient to overcome this factor, and this group actually appears to decrease the diatropic character of free base **15**. The UV-vis spectrum for **15** was typical of an azuliporphyrin, showing multiple bands in the Soret region and weaker broad absorptions at higher wavelengths (Figure 5). In TFA- CH_2Cl_2 , the corresponding dication 15H_2^{2+} gave a strong Soret-like band at 485 nm and several broadened Q bands between 600 and 800 nm (Figure 5).

Table 1. Selected Chemical Shifts (ppm) from the Proton NMR Spectra for Azuliporphyrins 15 and 16a,b in CDCl₃ and for the Corresponding Dications 15H₂²⁺ and 16a,bH₂²⁺ in TFA–CDCl₃^a



15, 16



15H₂²⁺, 16H₂²⁺

15 R = OMe
16a R = H
16b R = *t*-Bu

azuliporphyrin	5,20-H	10,15-H	12,13-H	2 ¹ ,3 ¹ -H	2 ² ,3 ² -H	21-H
15	9.06	8.99	8.79	9.35	7.52	2.93
16a	9.24	9.05	8.82	9.52	7.8–7.9	2.76
16b	9.33	9.14	8.88	9.56	8.11	2.33
15H₂²⁺	10.83	10.72	10.07	10.21	8.44	–4.24
16aH₂²⁺	10.86	10.60	9.99	10.38	8.92	–3.44
16bH₂²⁺	10.90	10.72	10.08	10.33	9.11	–3.92

^aThe data for 16a,b and 16a,bH₂²⁺ were taken from refs 2 and 4.

Scheme 9

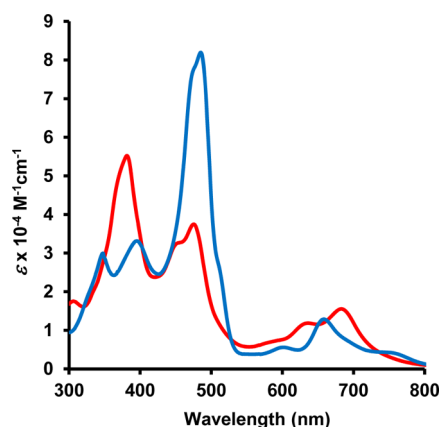
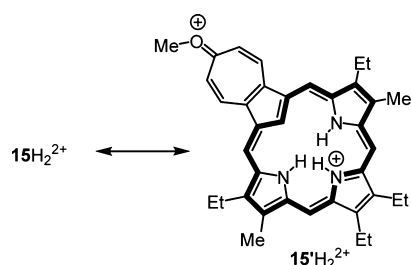


Figure 5. UV–vis spectra of methoxythiazuliporphyrin 15: free base in 1% Et₃N–CH₂Cl₂ (red line); dication 15H₂²⁺ in 1% TFA–CH₂Cl₂ (blue line).

Carbaporphyrins and related systems such as N-confused porphyrins readily form stable silver(III) complexes under mild conditions,^{24–28} and it was of some interest to see whether this type of complex could also be obtained from the tropone-fused carbaporphyrin 6. In fact, 6 reacted with silver(I) acetate in a mixture of dichloromethane and methanol to give the silver(III) organometallic complex 17 in 82% yield. The silver(III) derivative was poorly soluble in organic solvents, but a proton NMR spectrum could be obtained in CDCl₃. This showed the *meso* protons as two 2H singlets at 8.36 and 9.33 ppm, implying that the diatropic character of 17 is reduced in comparison to carbaporphyrin 6. Only a poor-quality carbon-13

NMR spectrum could be obtained, and it was not possible to identify the resonance for the carbonyl moiety. The IR spectrum for 17 showed carbonyl stretching at 1596 cm^{–1}, which is similar to the value recorded for 6. The UV–vis spectrum of 17 showed the presence of multiple peaks between 370 and 470 nm and a split absorption near 600 nm (Figure 6).

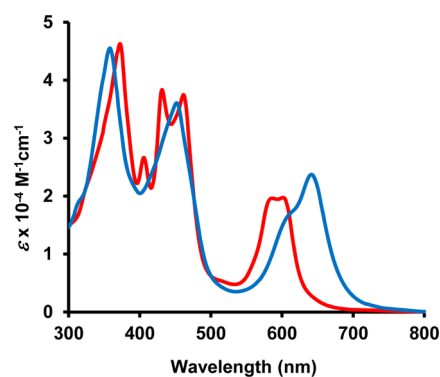
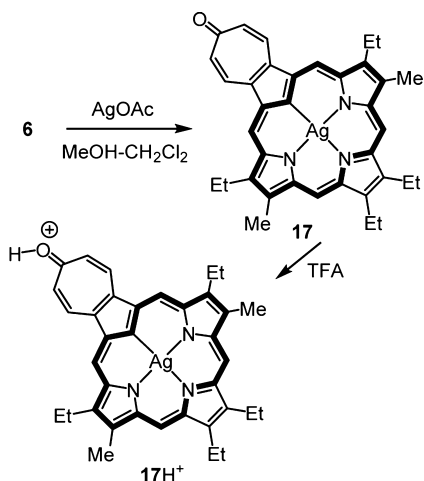


Figure 6. UV–vis spectra of silver(III) complex 17: free base in CH₂Cl₂ (red line); cation 17H⁺ in 1% TFA–CH₂Cl₂ (blue line).

Addition of TFA led to the formation of a new species attributed to cation 17H⁺ (Scheme 10), but this subsequently underwent demetalation. The insertion of silver(III) into the macrocycle was confirmed by high-resolution MALDI mass spectrometry.

In order to better understand these new systems, unsubstituted tropone-fused carbaporphyrins and related protonated and deprotonated species were assessed using density functional theory.²⁹ The carbaporphyrinoid structures were minimized using B3LYP/6-311++G(d,p). Although B3LYP has been shown to be very good at predicting porphyrinoid geometries and frequencies,^{30,31} the sensitivities of the relative energies to the choice of functionals needed to be assessed.^{32,33} In order to account for this issue, single point energy (SPE) calculations were performed on the minimized structures using M06-2X/6-311++G(d,p) and B3LYP-D/6-311++G(d,p).^{34,35} Several keto and hydroxy tautomers of tropone-fused carbaporphyrin (TFC) were considered. As there are two mobile protons in these structures, the tautomers

Scheme 10



are designated by the positions of these hydrogens. Keto tautomer **TFC-22,24-H** was calculated to be more than 5 kcal/mol more stable than **TFC-22,23-H** (Table 2). This difference is due to the latter species having fewer opportunities for hydrogen-bonding interactions. The hydroxyazuliporphyrin tautomer **TFC-O,23-H** was calculated to be between 14.60 and 15.73 kcal/mol less stable, while the related species **TFC-O,22-H** is even higher in energy (Table 2). The high-energy species **TFC-O,22-H** has two conformational minima where the OH can be oriented toward or away from the NH (designated L and R), but the difference in energy between these two structures was less than 0.1 kcal/mol. Tautomers **TFC-O,22-H-L/R** are higher in energy than the alternative hydroxy tautomer due to increased steric interactions between the internal hydrogens and diminished hydrogen bonding, in addition to unfavorable nitrogen lone pair/lone pair repulsions. The tropone-fused carbaporphyrin tautomers deviate significantly from planarity, while the hydroxyazuliporphyrins are nearly planar (Table 3). Nevertheless, the hydroxy forms are substantially less stable. It is worth pointing out at this stage that the same trends are observed for B3LYP, B3LYP-D, and M06-2X functionals, and ΔG values are also similar. The latter observation indicates that entropic factors are not significant when these porphyrinoid tautomers are compared. The consistency of these results also extends to the other species

Table 3. Angles (deg) between the Plane of Each of the Individual Rings (Pyrrole and Tropone) and the Overall Plane of the Macrocycle

molecule	<i>a</i>	<i>b</i>	<i>c</i>	<i>d</i>
TFC-22,24-H	9.29	6.52	6.55	6.53
TFC-22,23-H	7.00	3.94	6.89	9.53
TFC-O,23-H	0.02	0.01	0.02	0.01
TFC-O,22-H-L	0.00	0.01	0.01	0.02
TFC-O,22-H-R	0.00	0.01	0.01	0.02
TFC-O,22,24-H ⁺	10.07	7.18	7.11	7.18
TFC-O,22,23-H-L ⁺	7.44	4.79	7.74	10.35
TFC-O,22,23-H-R ⁺	7.41	4.74	7.71	10.32
TFC-22,23,24-H ⁺	9.92	13.87	18.99	13.87
TFCH ₂ ²⁺	9.50	13.98	19.06	13.96
[TFCa-H] ⁻	0.01	0.01	0.02	0.01
[TFCb-H] ⁻	0.00	0.03	0.01	0.02
[TFC-2H] ²⁻	0.00	0.00	0.00	0.00
23-S-TFC-22-H	3.82	2.62	6.35	9.42
23-S-TFC-OH	0.00	0.00	0.00	0.00
23-S-TFC-O,22-H-R ⁺	4.01	2.81	6.52	10.07
23-S-TFC-O,22-H-L ⁺	4.07	2.86	6.57	10.14
23-S-TFC-22,24-H ⁺	8.82	10.92	20.79	10.93
23-S-TFCH ₂ ²⁺	8.19	11.44	19.92	11.39
[23-S-TFC-H] ⁻	0.00	0.00	0.00	0.00

discussed below. Nucleus independent chemical shifts (NICS) were also calculated for these structures.³⁶ NICS calculations for the central position of the ring system allows the aromatic character of a porphyrinoid structure to be assessed, and a strongly negative value is associated with a highly diatropic species. **TFC-22,24-H** and the **22,23-H** tautomer gave the large negative values expected for highly diatropic species (Table 2), which is also consistent with the proton NMR spectrum obtained for **6** (Figure 2). As expected, the NICS(0) values for the hydroxyazuliporphyrin tautomers were much reduced but were still large enough (>-6) to imply the presence of a moderate diamagnetic ring current. NICS values were also calculated for the centers of individual rings, as these results can allow favored conjugation pathways to be identified.^{37,38} For **TFC-22,24-H**, pyrrole rings *b* and *d* gave NICS values of -12.61 , while the pyrrolenine ring *c* afforded a value of -2.99 (Table 2). Rings *a* and *e* gave low positive values. These results are consistent with the presence of an 18- π -electron

Table 2. Calculated Relative Energies (kcal/mol) and NICS Values (ppm) for Tautomers of Tropone-Fused Carbaporphyrin

Molecule	TFC-22,24-H	TFC-22,23-H	TFC-O,23-H	TFC-O,22-H-L	TFC-O,22-H-R
ΔG (B3LYP)	0.00	5.04	13.68	20.79	20.84
(B3LYP/M06-2X/B3LYP-D)	0.00/0.00/0.00	5.41/5.69/5.48	14.60/14.74/15.73	21.78/22.58/23.12	21.81/22.62/23.15
NICS(0)	-13.50	-12.87	-6.29	-6.59	-6.57
NICS(<i>a</i>)	+2.85	+5.28	-10.35	-11.26	-11.30
NICS(<i>b</i>)	-12.61	-3.11	-1.37	-0.44	-0.48
NICS(<i>c</i>)	-2.99	-12.34	-7.56	-0.71	-0.70
NICS(<i>d</i>)	-12.61	-13.92	-1.31	-7.56	-7.49
NICS(<i>e</i>)	+3.77	+3.76	+2.66	+2.52	+2.49

delocalization pathway where rings *b* and *d* lie within the [18]annulene subunit (see structure 18), but rings *a* and *c* fall outside of this pathway and are therefore deshielded. The low negative value for ring *c* may be due to minor contributions by dipolar canonical forms such as 19 (Figure 7) that could

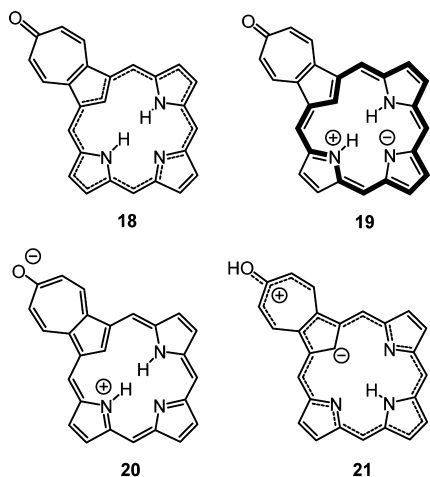


Figure 7. Selected conjugation pathways in tropone-fused carbaporphyrin tautomers.

provide a degree of shielding. The bond lengths calculated for TFC-22,24-H are also consistent with a favorable 18-atom 18- π -electron delocalization pathway (Figure 8). For instance, the

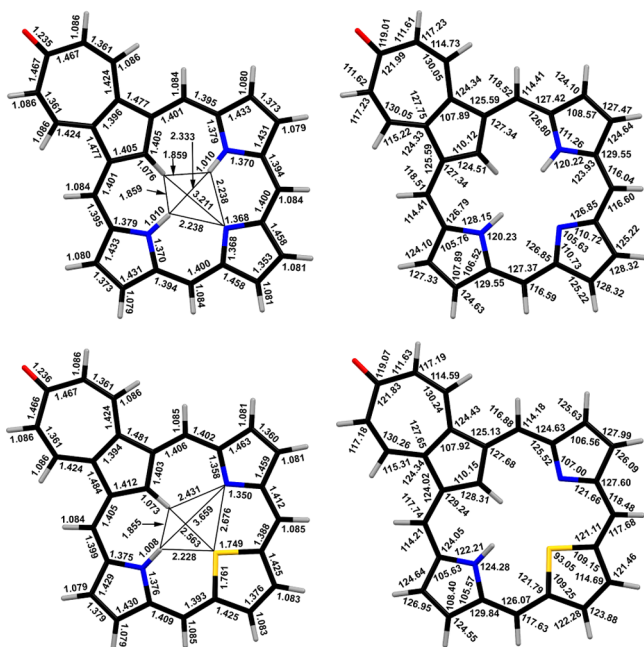


Figure 8. Bond lengths (Å) and angles (deg) for TFC-22,24-H and 23-S-TFC-22-H.

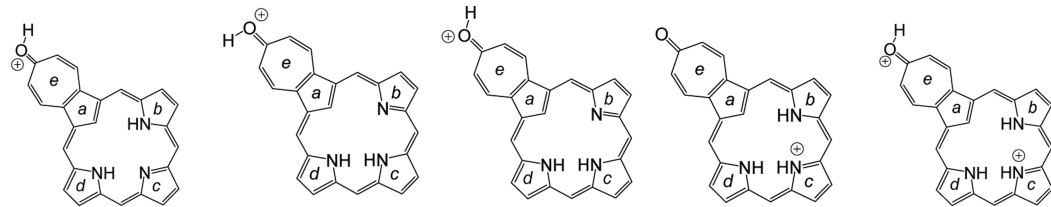
C1–C2, C3–C4, C11–C12, and C13–C14 bonds are relatively long, implying more single-bond character, in comparison to the C6–C7, C8–C9, C16–C17, and C18–C19 bonds that lie within the conjugation pathway. In addition, the C12–C13 bond is relatively short, suggesting that it has more double-bond character. The C=O bond length was calculated to be 1.235 Å. In the X-ray crystal structure for

tropone, two molecules were present per asymmetric unit and these gave bond lengths of 1.257 and 1.259 Å.³⁹ Hence, the C=O bond length in 6 is only slightly shorter than the value obtained for unsubstituted tropone. Enolate-like dipolar resonance contributors such as 20 do not appear to play a significant role. A similar analysis can be applied to TFC-22,23-H, although the [18]annulene pathway passes around rings *c* and *d* in this case. For hydroxyazuliporphyrin TFC-O,23-H, rings *a* and *c* are strongly shielded, while rings *b* and *d* give low negative values and the seven-membered ring *e* affords a low positive value. These results are not consistent with the proposed azuliporphyrin conjugation pathway 1x but fit the alternative dipolar species 21 (Figure 7). This proposed species should be considered in the same manner as a significant resonance contributor, rather than in isolation, but it is consistent with the proton NMR spectrum for methoxyazuliporphyrin 15. The same type of conjugation pathway can be proposed for TFC-O,22-H-L/R.

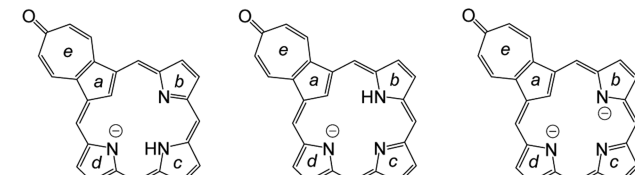
The formation of a monoprotonated species for tropone-fused carbaporphyrin 6 en route to the diprotonated dication $6H_2^{2+}$ was implied by the UV–vis data discussed earlier, but the structure of the monocation was not known. Three sites of protonation were considered (Table 4) to give TFC-22,23,24-H⁺, TFC-O,22,24-H⁺, or TFC-O,22,23-H⁺. In the last case, the OH can be oriented to the left or right to give two different conformational minima. Although we generally expect protonation to be favored on the imine nitrogen, the calculations clearly show that TFC-22,23,24-H⁺ is the least favorable option and the lowest energy form has been protonated on the carbonyl oxygen. TFC-O,22,24-H⁺ is lower in energy than the related tautomer TFC-O,22,23-H⁺ due to more favorable hydrogen-bonding interactions within the macrocyclic cavity, although this structure is far from planar (Table 2). The NICS(0) value for the lowest energy form is –10.65, indicating that this species retains substantial diatropic character. Although the hydroxyazuliporphyrin-type resonance contributor 22 (Figure 9) can be written for this species, the NICS data are not consistent with this structure. Rings *a*, *b*, and *d* give significantly negative NICS values, but rings *c* and *e* give values close to 0. These results would seem to favor a 19-atom delocalization pathway, as illustrated for structure 23 (Figure 9). The diprotonated species TFC-H₂²⁺ is further distorted away from planarity (Table 2) but still gives a NICS(0) value of –11.76 (Table 4). Rings *b*–*d* all give NICS values of >–12, but rings *a* and *e* give negligible shifts. These results suggest that the dication favors the 19-atom delocalization pathway found in structure 24 (Figure 9).

The corresponding deprotonated carbaporphyrinoids were also considered. Two tautomeric monoanions, [TFCa-H][–] and [TFCb-H][–], were considered, and the former was shown to be 3.69–3.74 kcal/mol more stable due to reduced steric crowding and improved hydrogen-bonding interactions within the macrocyclic cavity (Table 4). Both forms are essentially planar (Table 2). The NICS(0) value for the favored monoanion was –11.21, in keeping with the proton NMR spectrum obtained for [6-H][–]. For the individual rings, only ring *c* gave a significantly negative NICS value, suggesting that a 17-atom delocalization pathway is favored for this species (structure 25). Enolate-type contributors such as 26 do not appear to be significant. For the dianion [TFC-2H]^{2–}, the NICS(0) value is –9.40, but none of the individual rings show significant shielding. This result implies that the 16-atom delocalization pathway shown in structure 27 is favored (Figure 9).

Table 4. Calculated Relative Energies (kcal/mol) and NICS Values (ppm) for Protonated and Deprotonated Tropone-Fused Carbaporphyrins



Molecule	TFC-O,22,24-H ⁺	TFC-O,22,23-H-L ⁺	TFC-O,22,23-H-R ⁺	TFC-22,23,24-H ⁺	TFC-H ₂ ²⁺
ΔG (B3LYP)	0.00	3.44	3.37	10.69	*****
(B3LYP/M06-2X/B3LYP-D)	0.00/0.00/0.00	3.70/3.69/3.74	3.68/3.67/3.72	11.27/10.14/9.81	*****
NICS(0)	-10.65	-9.81	-9.80	-13.35	-11.76
NICS(a)	-7.59	-5.53	-5.56	+7.61	-0.85
NICS(b)	-9.95	-1.56	-1.61	-13.72	-12.32
NICS(c)	-0.51	-9.75	-9.74	-14.03	-12.19
NICS(d)	-9.90	-11.09	-11.03	-13.72	-12.27
NICS(e)	-0.02	+0.44	+0.45	+4.22	-0.96



Molecule	[TFCa-H] ⁻	[TFCb-H] ⁻	[TFC-2H] ²⁻
ΔG (B3LYP)	0.00	5.90	*****
(B3LYP/M06-2X/B3LYP-D)	0.00/0.00/0.00	5.95/6.49/6.15	*****
NICS(0)	-11.21	-11.58	-9.40
NICS(a)	+3.04	+1.92	-2.23
NICS(b)	-3.62	-11.55	-2.82
NICS(c)	-11.01	-2.83	-1.85
NICS(d)	-3.62	-2.54	-2.82
NICS(e)	+3.39	+3.39	+4.14

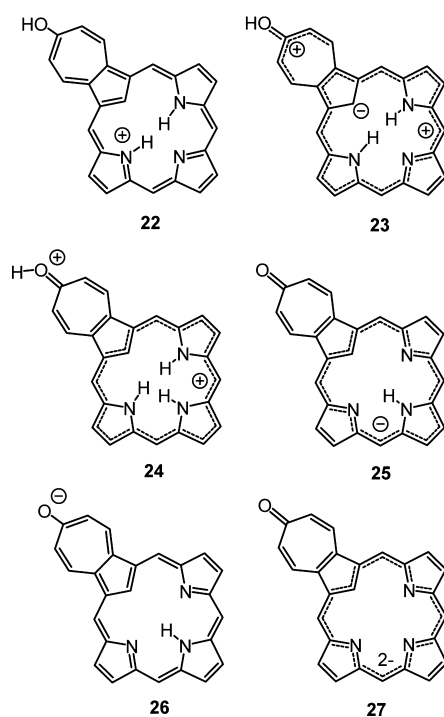
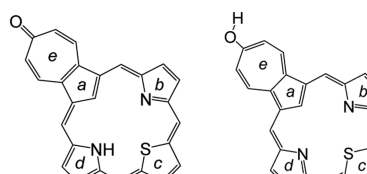


Figure 9. Selected conjugation pathways in protonated and deprotonated tropone-fused carbaporphyrins.

Two tautomers were considered for tropone-fused 23-thiacarporphyrin (**23-S-TFC**) (Table 5). As expected, the keto form **23-S-TFC-22-H** was between 11.05 and 12.64 kcal/mol more stable than the hydroxythiazulporphyrin structure **23-S-TFC-OH**. Nevertheless, the latter structure is completely planar, while the more stable form is significantly twisted away from planarity (Table 2). **23-S-TFC-22-H** has a NICS(0) value of -13.43 , which is consistent with the highly diatropic

Table 5. Calculated Relative Energies (kcal/mol) and NICS Values (ppm) for Tautomers of Tropone-Fused 23-Thiacarporphyrin



Molecule	23-S-TFC-22-H	23-S-TFC-OH
ΔG (B3LYP)	0.00	11.17
(B3LYP/M06-2X/B3LYP-D)	0.00/0.00/0.00	11.62/11.05/12.64
NICS(0)	-13.43	-7.47
NICS(a)	+6.61	-9.65
NICS(b)	-1.43	-0.97
NICS(c)	-15.71	-8.37
NICS(d)	-13.53	-0.91
NICS(e)	+3.78	+1.55

characteristics observed in the proton NMR spectrum of **14**. For the individual rings, only rings *c* and *d* gave large negative values and this is consistent with a favored 18-atom delocalization pathway (structure **28**, Figure 10). This

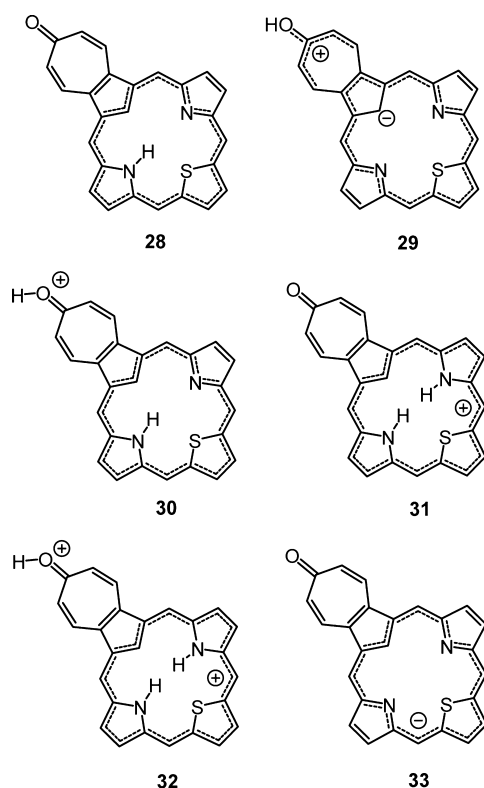


Figure 10. Selected conjugation pathways in troponone-fused thiocarbaporphyrin tautomers and related protonated and deprotonated species.

interpretation is also supported by an analysis of the calculated bond lengths for **21-S-TFC-22-H** (Figure 8). The calculated C=O bond length of 1.236 Å is similar to the value obtained for **TFC-22,24-H**. The hydroxythiazuliporphyrin tautomer **23-S-TFC-OH** gave a moderate NICS(*a*) value of -7.47 , and only rings *a* and *c* showed significant shielding. This is consistent with contributions from dipolar structure **29** (Figure 10). Two

monoprotonated species were considered, **23-S-TFC-O,22-H⁺** and **23-TFC-22,24-H⁺**, and again protonation onto the carbonyl oxygen was favored (Table 6). For the favored tautomer, two conformational minima were noted where the OH was oriented to the left or right, but the difference in energy was only 0.01–0.03 kcal/mol. The NICS(*a*) value was -10.77 , and rings *c* and *d* also showed large negative NICS values. These data indicate that the 18-atom delocalization pathway shown in structure **30** is favored (Figure 10). The N-protonated monocation **23-S-TFC-22,24-H** is only 3.39–4.66 kcal/mol higher in energy in this case and shows a larger NICS(0) value, although steric crowding leads to a significant loss of planarity (Table 3). The NICS data show that rings *b–d* are strongly shielded (Table 6), and this is consistent with the presence of a 19-atom delocalization pathway (structure **31**). The dication **23-S-TFC-H₂²⁺** is also nonplanar (Table 3) but gives a strongly aromatic NICS(0) value of -12.70 . Rings *b–d* show substantial shielding, implying that the dication also favors a 19-atom delocalization pathway (structure **32**). The deprotonated species **[23-S-TFC-H]⁻** was also considered, and this species shows a NICS(0) value of -11.82 , supporting the results obtained from the proton NMR spectrum of **[14-H]⁻** in DBU-CDCl₃. This species is planar, due to the presence of only one hydrogen atom within the macrocyclic cavity. Only ring *c* shows a significantly shielded NICS value, and this suggests that the anion favors the 17-atom delocalization pathway shown in structure **33** (Figure 10).

CONCLUSIONS

Acid-catalyzed condensation of a methoxyazulitripyrrane with a pyrrole dialdehyde, followed by oxidation with aqueous ferric chloride, gave an unusual troponone-fused carbaporphyrin, and a similar thiocarbaporphyrinoid was prepared using the same approach. These porphyrins exhibited strongly diatropic characteristics, but the UV–vis spectra were somewhat modified, showing multiple bands in the Soret region that resemble the spectra obtained for azuliporphyrins. Protonation affords diprotonated species that also retain aromatic characteristics. UV–vis spectroscopic titrations indicate that transient monoprotonated structures are formed, and DFT calculations demonstrated that O protonation is favored over N protonation. In the presence of DBU, deprotonation occurred to generate aromatic anions. The troponone-fused carbaporphyrin

Table 6. Calculated Relative Energies (kcal/mol) and NICS Values (ppm) for Protonated and Deprotonated Troponone-Fused Thiocarbaporphyrins

Molecule	23-S-TFC-O,22-H-R	23-S-TFC-,22-H-L	23-S-TFC-22,24-H	23-S-TFC-H₂²⁺	[23-S-TFC-H]⁻
ΔG (B3LYP)	0.00	0.06	4.31	*****	*****
(B3LYP/M06-2X/B3LYP-D)	0.00/0.00/0.00	0.03/0.01/0.02	4.66/4.00/3.39	*****	*****
NICS(0)	-10.77	-10.77	-14.00	-12.70	-11.82
NICS(<i>a</i>)	-4.25	-4.23	+8.82	-0.18	+2.99
NICS(<i>b</i>)	-0.15	-0.10	-12.92	-11.66	-3.03
NICS(<i>c</i>)	-12.84	-12.84	-17.72	-15.90	-12.53
NICS(<i>d</i>)	-10.82	-10.89	-12.92	-11.61	-3.03
NICS(<i>e</i>)	+0.20	+0.21	+4.36	-0.91	+3.31

also reacted with silver(I) acetate to give a silver(III) derivative. NICS calculations were employed to examine these porphyrinoids, related tautomers, protonated species, and anionic structures, and these results allowed favorable delocalization pathways to be identified. It can be concluded that the presence of a fused tropone unit drastically modifies the properties of the carbaporphyrin core.

EXPERIMENTAL SECTION

Melting points are uncorrected. IR spectra were obtained on a FT-IR spectrometer equipped with an attenuated total reflectance (ATR) diamond cell. NMR spectra were recorded using a 400 or 500 MHz NMR spectrometer and were run at 300 K unless otherwise indicated. ^1H NMR values are reported as chemical shifts δ , relative integral, multiplicity (s, singlet; d, doublet; t, triplet; q, quartet; m, multiplet; br, broad peak), and coupling constant (J). Chemical shifts are reported in parts per million (ppm) relative to CDCl_3 (^1H residual CHCl_3 δ 7.26, ^{13}C CDCl_3 triplet δ 77.23), and coupling constants were taken directly from the spectra. NMR assignments were made with the aid of ^1H - ^1H COSY, HSQC, DEPT-135, and NOE difference proton NMR spectroscopy. 2D experiments were performed by using standard software. High-resolution mass spectra (HRMS) were carried out by using a double-focusing magnetic sector instrument. ^1H and ^{13}C NMR spectra for all new compounds are reported in the Supporting Information.

1,3-Bis(5-tert-butylcarbonyl-3-ethyl-4-methyl-2-pyrrolyl-methyl)-6-methoxyazulene (11). 6-Methoxyazulene¹⁶ (540 mg, 3.42 mmol) and *tert*-butyl 5-acetoxymethyl-4-ethyl-3-methylpyrrole-2-carboxylate³⁹ (1.93 g, 6.87 mmol) were dissolved in ethanol (50 mL) and acetic acid (10 mL). The mixture was flushed with nitrogen and stirred under reflux overnight. The solvent was evaporated under reduced pressure and the residue purified on a silica gel column with 20% hexanes–dichloromethane as eluent. A major purple band was collected corresponding to the tripyrrane analogue. The solvent was evaporated and the residue recrystallized from hexanes to give **12** (1.47 g, 2.45 mmol, 72%) as blue crystals: mp 154–155 °C with softening at 82–84 °C; ^1H NMR (500 MHz, CDCl_3) δ 1.08 (6H, t, J = 7.5 Hz, 2 \times CH_2CH_3), 1.48 (18H, s, 2 \times *t*-Bu), 2.26 (6H, s, 2 \times pyrrole- CH_3), 2.49 (4H, q, J = 7.5 Hz, 2 \times CH_2CH_3), 3.92 (3H, s, OCH_3), 4.25 (4H, s, 2 \times bridge- CH_2), 6.68 (2H, d, J = 11.0 Hz, 5,7-H), 7.21 (1H, s, 2-H), 8.02 (2H, d, J = 11.0 Hz, 4,8-H), 8.16 (2H, br s, 2 \times NH); ^{13}C NMR (CDCl_3) δ 10.8 (2 \times pyrrole- CH_3), 15.7 (2 \times CH_2CH_3), 17.6 (2 \times CH_2CH_3), 24.3 (2 \times bridge- CH_2), 28.7 ($\text{C}(\text{CH}_3)_3$), 56.1 (OCH_3), 80.2 ($\text{C}(\text{CH}_3)_3$), 109.4 (5,7-CH), 118.6, 123.3, 125.8, 126, 131.8, 133.0 (4,8-CH), 134.3 (2-CH), 161.6 (6-C), 167.9 (2 \times $\text{C}=\text{O}$); HR MS (EI) calcd for $\text{C}_{37}\text{H}_{48}\text{N}_2\text{O}_5$ 600.3563, found 600.3581. Anal. Calcd for $\text{C}_{37}\text{H}_{48}\text{N}_2\text{O}_5$: C, 73.97; H, 8.05; N, 4.66. Found: C, 74.13; H, 8.21; N, 4.71.

Tropone-Fused Carbaporphyrin 6. Azulitripyrrane **12** (96.0 mg, 0.16 mmol) was stirred with TFA (4 mL) under nitrogen for 10 min. The reaction mixture was diluted with dichloromethane (100 mL), 3,4-diethylpyrrole-2,5-dicarbaldehyde^{17,18} (29.0 mg, 0.16 mg) was added, and the mixture was stirred overnight in the dark at room temperature. The solution was vigorously shaken with 0.1% aqueous ferric chloride solution (150 mL) for 7–8 min, the organic layer was separated, and the aqueous solution was back-extracted with chloroform. The combined organic solutions were washed with water and 5% aqueous sodium bicarbonate solution and dried over sodium sulfate. The solvent was removed under reduced pressure, and the residue was run through a grade 3 basic alumina column, with chloroform as eluent. A brown prefraction was noted that corresponded to a complex mixture of carbaporphyrin byproducts. The major fraction was further purified on a silica gel column, with chloroform and then 1% methanol–chloroform and 2% methanol–chloroform as eluents. The product was collected as a green fraction. Recrystallization from chloroform–hexanes gave the tropone-fused carbaporphyrin (27.5 mg, 0.052 mmol, 32%) as dark purple crystals: mp >300 °C; UV–vis (1% $\text{Et}_3\text{N}-\text{CH}_2\text{Cl}_2$) λ_{max} (log ϵ) 337 (sh, 4.58), 377 (4.83), 412 (4.79), 436 (4.86), 458 (sh, 4.83), 503 (sh, 4.12), 533

(4.14), 578 (4.54), 650 (3.70), 715 nm (3.42); UV–vis (1% TFA- CH_2Cl_2) λ_{max} (log ϵ) 343 (sh, 4.65), 372 (4.83), 461 (5.06), 500 (sh, 4.48), 570 (3.84), 629 (4.42), 676 (sh, 4.01), 736 nm (sh, 3.76); UV–vis (5% DBU- CH_2Cl_2) λ_{max} (log ϵ) 352 (4.71), 388 (4.70), 481 (4.98), 536 (sh, 4.11), 597 (4.01), 657 nm (4.39); IR $\nu_{\text{C}=\text{O}}$ 1596 cm^{-1} ; ^1H NMR (500 MHz, CDCl_3) δ -7.64 (1H, s, 21-H), -4.47 (2H, br, 2 \times NH), 1.70 (6H, t, J = 7.7 Hz, 7,18- CH_2CH_3), 1.84 (6H, t, J = 7.7 Hz, 12,13- CH_2CH_3), 3.42 (6H, s), 3.79 (4H, q, J = 7.7 Hz, 7,18- CH_2), 3.86 (4H, q, J = 7.7 Hz, 12,13- CH_2), 7.37 (2H, d, J = 11.2 Hz, 2',3',2'-H), 8.47 (2H, d, J = 11.2 Hz, 2',3',1'-H), 9.26 (2H, s, 5,20-H), 9.40 (2H, s, 10,15-H); ^{13}C NMR (125 MHz, CDCl_3) δ 11.0 (8,17- CH_3), 17.3 (7,18- CH_2CH_3), 18.6 (12,13- CH_2CH_3), 19.6 (7,18- CH_2), 20.0 (12,13- CH_2), 95.1 (10,15-CH), 100.0 (5,20-CH), 102.6 (21-CH), 130.4, 130.7, 131.1 (2',3',1'-CH), 133.5, 136.3 (2',3',2'-CH), 138.9, 139.5, 141.4, 145.3, 155.3, 188.1 ($\text{C}=\text{O}$); ^1H NMR (500 MHz, TFA- CDCl_3 , dication 6H_2^{2+}) δ -4.40 (1H, s, 21-H), -2.60 (1H, v br, 23-H), -0.68 (2H, br, 22,24-NH), 1.68 (6H, t, J = 7.7 Hz, 7,18- CH_2CH_3), 1.82 (6H, t, J = 7.7 Hz, 12,13- CH_2CH_3), 3.45 (6H, s, 8,17- CH_3), 3.94–4.01 (4H, m, 4 \times CH_2CH_3), 8.23 (2H, d, J = 10.8 Hz, 2',3',2'-H), 9.73 (2H, d, J = 10.8 Hz, 2',3',1'-H), 9.74 (2H, s, 10,15-H), 10.38 (2H, s, 5,20-H); ^{13}C NMR (125 MHz, TFA- CDCl_3 , dication 6H_2^{2+}) δ 11.5 (8,17- CH_3), 16.7 (7,18- CH_2CH_3), 17.4 (12,13- CH_2CH_3), 19.8, 20.1 (4 \times CH_2CH_3), 95.5 (10,15-CH), 109.1 (5,20-CH), 118.9 (21-CH), 130.1, 132.6 (2',3',2'-CH), 135.4, 139.8 (2',3',1'-CH), 140.6, 142.1, 144.2, 145.5, 147.2, 148.8, 177.5; ^1H NMR (500 MHz, 323 K, DBU- CDCl_3 , anion $[6\text{-H}]^-$, upfield and downfield regions only) δ -6.45 (1H, br s, 21-H), 7.26 (2H, d, J = 11.3 Hz), 8.59 (2H, d, J = 11.3 Hz), 9.28 (2H, s), 9.42 (2H, s); HR MS (ESI) calcd for $\text{C}_{36}\text{H}_{37}\text{N}_3\text{O} + \text{H}$ 528.3015, found 528.3009.

Tropone-Fused Thiaporphyrin 14. Under the same conditions as the foregoing reaction, azulitripyrrane (96.0 mg, 0.16 mmol) was reacted with thiophene-2,5-dicarbaldehyde (22.4 mg, 0.16 mmol). Recrystallization from chloroform–hexanes gave the tropone-fused thiaporphyrin (11.4–24.0 mg, 0.023–0.049 mmol, 15–31%) as dark purple crystals: mp >300 °C; UV–vis (CH_2Cl_2) λ_{max} (log ϵ) 406 (4.58), 446 (4.58), 552 (3.94), 595 (4.05), 743 nm (3.34); UV–vis (1% TFA- CH_2Cl_2) λ_{max} (log ϵ) 341 (4.42), 424 (4.59), 465 (4.76), 584 (3.92), 641 nm (3.91); UV–vis (1% DBU- CH_2Cl_2) λ_{max} (log ϵ) 356 (4.42), 392 (4.46), 480 (4.68), 605 (3.81), 664 nm (4.14); IR $\nu_{\text{C}=\text{O}}$ 1591 cm^{-1} ; ^1H NMR (500 MHz, CDCl_3 , 323 K) δ -6.79 (1H, s, 21-H), -4.7 (1H, v br), 1.67 (6H, t, J = 7.7 Hz, 2 \times CH_2CH_3), 3.23 (6H, s, 8,17- CH_3), 3.60 (4H, q, J = 7.7 Hz, 7,18- CH_2), 7.41 (2H, d, J = 11.3 Hz, 2',3',2'-H), 8.42 (2H, d, J = 11.3 Hz, 2',3',1'-H), 9.17 (2H, s, 12,13-H), 9.56 (2H, s, 10,15-H), 9.89 (2H, s, 5,20-H); ^{13}C NMR (125 MHz, CDCl_3 , 323 K) δ 11.1 (8,17- CH_3), 17.4 (2 \times CH_2CH_3), 19.6 (7,18- CH_2), 107.1 (5,20-CH), 108.4 (10,15-CH), 111.7 (21-CH), 131.0 (2',3',1'-CH), 133.0 (12,13-CH), 133.4, 134.1, 137.3 (2',3',2'-CH), 137.5, 142.6, 143.4, 144.1, 148.9, 187.9 ($\text{C}=\text{O}$); ^1H NMR (500 MHz, TFA- CDCl_3 , dication 14H_2^{2+}) δ -4.73 (1H, s, 21-H), -2.51 (2H, br s, 2 \times NH), 1.78 (6H, t, J = 7.7 Hz, 2 \times CH_2CH_3), 3.54 (6H, s), 4.08 (4H, q, J = 7.7 Hz, 7,18- CH_2), 8.51 (2H, d, J = 11.0 Hz, 2',3',2'-H), 10.02 (2H, d, J = 11.0 Hz, 2',3',1'-H), 10.10 (2H, s, 12,13-H), 10.76 (2H, s), 10.77 (2H, s) (4 \times *meso*-H); ^{13}C NMR (125 MHz, TFA- CDCl_3 , dication 14H_2^{2+}) δ 11.6 (8,17- CH_3), 16.8 (2 \times CH_2CH_3), 20.1 (7,18- CH_2), 110.9, 111.1 (4 \times *meso*-CH), 117.3, 132.8, 134.4 (2',3',2'-CH), 137.6, 138.6 (12,13-CH), 140.35, 140.39 (2',3',1'-CH), 140.8, 146.5, 148.3, 150.6, 179.1; ^1H NMR (500 MHz, 323 K, DBU- CDCl_3 , anion $[14\text{-H}]^-$, 323 K, upfield and downfield regions only) δ -3.08 (1H, br s, 21-H), 7.41 (2H, d, J = 11.4 Hz), 9.10 (2H, d, J = 11.4 Hz), 9.41 (2H, s), 9.83 (2H, s), 9.86 (2H, s); HR MS (EI) calcd for $\text{C}_{32}\text{H}_{28}\text{N}_2\text{OS}$ 488.1931, found 488.1922.

7,18-Diethyl-2³-methoxy-8,17-dimethyl-23-thiaazuliporphyrin (15). In the foregoing experiment, a green band eluted from the alumina column with 5% methanol–chloroform. Recrystallization from chloroform–hexanes afforded the thiaazuliporphyrin (10.3–22.2 mg, 0.020–0.044 mmol, 13–28%) as a dark green powder: mp >300 °C; UV–vis (1% $\text{Et}_3\text{N}-\text{CH}_2\text{Cl}_2$) λ_{max} (log ϵ) 381 (4.74), 450 (sh, 4.51), 475 (4.57), 633 (sh, 4.07), 683 nm (4.19); UV–vis (1% TFA- CH_2Cl_2) λ_{max} (log ϵ) 348 (4.47), 395 (4.52), 475 (sh, 4.89), 485 (4.91), 601 (3.74), 658 (4.11), 753 nm (sh, 3.62); ^1H NMR (500

MHz, CDCl₃) δ 1.56 (6H, t, $J = 7.7$ Hz, $2 \times \text{CH}_2\text{CH}_3$), 2.94 (6H, s, 8,17-CH₃), 3.49 (4H, q, $J = 7.7$ Hz, 7,18-CH₂), 4.26 (3H, s, OCH₃), 7.52 (2H, d, $J = 10.6$ Hz), 8.79 (2H, s), 8.99 (2H, s), 9.06 (2H, s), 9.35 (2H, d, $J = 10.6$ Hz); ¹H NMR (500 MHz, TFA-CDCl₃, dication 15H₂²⁺) δ -4.24 (1H, s, 21-H), -2.2 (2H, v br), 1.77 (6H, t, $J = 7.7$ Hz, $2 \times \text{CH}_2\text{CH}_3$), 3.52 (6H, s, 8,17-CH₃), 4.07 (4H, q, $J = 7.7$ Hz, 7,18-CH₂), 4.47 (3H, s, OCH₃), 8.44 (2H, d, $J = 11.0$ Hz, 2²,3²-H), 10.07 (2H, s, 12,13-H), 10.21 (2H, d, $J = 11.0$ Hz, 2¹,3¹-H), 10.72 (2H, s, 10,15-H), 10.83 (2H, s, 5,20-H); ¹³C NMR (125 MHz, TFA-CDCl₃, dication 15H₂²⁺) δ 11.5 (8,17-CH₃), 16.6 ($2 \times \text{CH}_2\text{CH}_3$), 20.1 (7,18-CH₂), 58.9 (OCH₃), 111.1 (10,15-CH), 112.0 (5,20-CH), 118.6 (21-CH), 131.1 (2²,3²-CH), 131.9, 137.7, 139.0 (12,13-CH), 140.86, 140.90 (2¹,3¹-CH), 147.4, 148.8, 149.2, 151.4, 176.6; HR MS (ESI) calcd for C₃₃H₃₀N₂O⁺ + H 503.2152, found 503.2159.

Silver(III) Complex 17. A suspension of silver(I) acetate (10 mg, 0.06 mmol) in methanol (5 mL) was added to a stirred solution of tropone-fused carbaporphyrin **14** (10.0 mg, 0.019 mmol) in dichloromethane (5 mL), and the mixture was stirred at room temperature overnight. The solution was washed with water and the solvent removed under reduced pressure. The residue was purified by column chromatography on grade 3 alumina with chloroform as eluent. Recrystallization from chloroform-methanol gave the silver-(III) complex (9.9 mg, 0.016 mmol, 82%) as a dark purple solid: mp >300 °C; UV-vis (1% TEA-CH₂Cl₂) λ_{max} (log ϵ) 372 (4.66), 406 (4.43), 431 (4.59), 461 (4.57), 584 (4.29), 601 nm (4.30); UV-vis (1% TFA-CH₂Cl₂) λ_{max} (log ϵ) 358 (4.66), 452 (4.56), 609 (sh, 4.22), 641 nm (4.37); IR $\nu_{\text{C=O}}$ 1595 cm⁻¹; ¹H NMR (500 MHz, CDCl₃) δ 1.92 (12H, t, $J = 7.8$ Hz), 3.29 (6H, s), 3.45 (4H, q, $J = 7.7$ Hz), 3.96 (4H, q, $J = 7.8$ Hz), 7.32 (2H, d, $J = 11.0$ Hz), 7.93 (2H, d, $J = 11.0$ Hz), 8.36 (2H, s), 9.33 (2H, s); ¹³C NMR (125 MHz, CDCl₃, 323 K) δ 11.7, 17.2, 18.3, 19.5, 19.9, 97.2, 102.9, 131.0, 132.7, 133.3, 134.5, 138.1, 138.4, 138.9, 140.4, 141.8; HR-MS (MALDI) calcd for C₃₆H₃₄AgN₃O + H 632.1824, found 632.1835.

Computational Studies. All calculations were performed using Gaussian 09⁴⁰ Rev D.01 running on a Linux-based PC. Energy minimization and frequency calculations of the porphyrinoid systems were performed at the density functional theory (DFT) level of theory with the B3LYP functional and a 6-311++G(d,p) basis set. Single point energy calculations were performed on the minimized structures using both the B3LYP-D and M062-X functionals and a 6-311++G(d,p) basis set. Mercury 3.1 running on an OS X platform, as provided by the CCDC (www.ccdc.cam.ac.uk/mercury/), was used to visualize the optimized structures. The resulting Cartesian coordinates of the molecules can be found in the Supporting Information.

NICS values were computed using the GIAO method,⁴¹ at the DFT level with the B3LYP functional and a 6-31+G(d,p) basis set, at several positions in each molecule. NICS(0) was calculated at the mean position of all the heavy atoms. NICS(a), NICS(b), NICS(c), NICS(d), and NICS(e) values were obtained by applying the same method to the mean position of the heavy atoms that comprise the individual rings of each macrocycle.

■ ASSOCIATED CONTENT

● Supporting Information

Figures and tables giving selected ¹H NMR, ¹H-¹H COSY, HSQC, DEPT-135, ¹³C NMR, MS, and UV-vis spectra and calculated structures and Cartesian coordinates. This material is available free of charge via the Internet at <http://pubs.acs.org>.

■ AUTHOR INFORMATION

Corresponding Author

*E-mail for T.D.L.: tdlash@ilstu.edu.

Notes

The authors declare no competing financial interest.

■ ACKNOWLEDGMENTS

This work was supported by the National Science Foundation under Grant No. CHE-1212691 and the donors of the Petroleum Research Fund, administered by the American Chemical Society.

■ REFERENCES

- (1) Lash, T. D.; Chaney, S. T. *Angew. Chem., Int. Ed.* **1997**, *36*, 839–840.
- (2) Lash, T. D.; Colby, D. A.; Graham, S. R.; Chaney, S. T. *J. Org. Chem.* **2004**, *69*, 8851–8864.
- (3) Lash, T. D.; El-Beck, J. A.; Ferrence, G. M. *J. Org. Chem.* **2007**, *72*, 8402–8415.
- (4) Lash, T. D.; El-Beck, J. A.; Ferrence, G. M. *Org. Biomol. Chem.* **2014**, *12*, 316–329.
- (5) (a) Lash, T. D. In *Handbook of Porphyrin Science-With Applications to Chemistry, Physics, Material Science, Engineering, Biology and Medicine*; Kadish, K. M., Smith, K. M., Guillard, R., Eds.; World Scientific Publishing: Singapore, 2012; Vol. 16, pp 1–329. (b) Medforth, C. J. In *The Porphyrin Handbook*; Kadish, K. M., Smith, K. M., Guillard, R., Eds.; Academic Press: San Diego, CA, 2000; Vol. 5, pp 1–80.
- (6) (a) Colby, D. A.; Lash, T. D. *Chem. Eur. J.* **2002**, *8*, 5397–5402. (b) Lash, T. D.; Colby, D. A.; Ferrence, G. M. *Eur. J. Org. Chem.* **2003**, 4533–4548.
- (7) Okujima, T.; Kikkawa, T.; Nakano, H.; Kubota, H.; Fukugami, N.; Ono, N.; Yamada, H.; Uno, H. *Chem. Eur. J.* **2012**, *18*, 12854–12863.
- (8) Lash, T. D. *Chem. Commun.* **1998**, 1683–1684.
- (9) (a) Graham, S. R.; Ferrence, G. M.; Lash, T. D. *Chem. Commun.* **2002**, 894–895. (b) Lash, T. D.; Colby, D. A.; Graham, S. R.; Ferrence, G. M.; Szczepura, L. F. *Inorg. Chem.* **2003**, *42*, 7326–7338.
- (10) Lash, T. D.; Pokharel, K.; Zeller, M.; Ferrence, G. M. *Chem. Commun.* **2012**, 48, 11793–11795.
- (11) Bialek, M.; Latos-Grazynski, L. *Chem. Commun.* **2014**, *50*, 9270–9272.
- (12) Colby, D. A.; Ferrence, G. M.; Lash, T. D. *Angew. Chem., Int. Ed.* **2004**, *43*, 1346–1349.
- (13) El-Beck, J. A.; Lash, T. D. *Eur. J. Org. Chem.* **2007**, 3981–3990.
- (14) Lash, T. D.; Gilot, G. C. Presented in part at the 246th ACS National Meeting, Indianapolis, IN, September 11, 2013; Abstracts of Papers, ORGN-323.
- (15) Graham, S. R.; Colby, D. A.; Lash, T. D. *Angew. Chem., Int. Ed.* **2002**, *41*, 1371–1374.
- (16) McDonald, R. N.; Richmond, J. M.; Curtis, J. R.; Petty, H. E.; Hoskins, T. L. *J. Org. Chem.* **1976**, *41*, 1811–1821.
- (17) Tardieux, C.; Bolze, F.; Gros, C. P.; Guillard, R. *Synthesis* **1998**, 267–268.
- (18) Li, R.; Lammer, A. D.; Ferrence, G. M.; Lash, T. D. *J. Org. Chem.* **2014**, *79*, 4078–4093.
- (19) An example of a carbaporphyrin with an unsubstituted cyclopentadiene ring was recently reported, and this also shows several medium-sized absorptions in the Soret band region: Li, D.; Lash, T. D. *J. Org. Chem.* **2014**, *79*, 7112–7121.
- (20) Badger, G. M. *Aromatic Character and Aromaticity*; Cambridge University Press: London, 1969.
- (21) Lash, T. D.; Hayes, M. J. *Angew. Chem., Int. Ed. Engl.* **1997**, *36*, 840–842.
- (22) Lash, T. D.; Hayes, M. J.; Spence, J. D.; Muckey, M. A.; Ferrence, G. M.; Szczepura, L. F. *J. Org. Chem.* **2002**, *67*, 4860–4874.
- (23) (a) Lash, T. D. *Synlett* **2000**, 279–295. (b) Lash, T. D. *Eur. J. Org. Chem.* **2007**, 5461–5481.
- (24) Lash, T. D. *Chem. Asian J.* **2014**, *9*, 682–705.
- (25) Furuta, H.; Ogawa, T.; Uwatoko, Y.; Araki, K. *Inorg. Chem.* **1999**, *38*, 2676–2682.
- (26) Muckey, M. A.; Szczepura, L. F.; Ferrence, G. M.; Lash, T. D. *Inorg. Chem.* **2002**, *41*, 4840–4842.

- (27) Lash, T. D.; Colby, D. A.; Szczepura, L. F. *Inorg. Chem.* **2004**, *43*, 5258–5267.
- (28) Lash, T. D.; Rasmussen, J. M.; Bergman, K. M.; Colby, D. A. *Org. Lett.* **2004**, *6*, 549–552.
- (29) (a) Ghosh, A. *Acc. Chem. Res.* **1998**, *31*, 189–198. (b) Ghosh, A. in *The Porphyrin Handbook*; Kadish, K. M., Smith, K. M., Guillard, R., Eds.: Academic Press: San Diego, CA, 2000; Vol. 7, pp 1–38.
- (30) Alonso, M.; Geerlings, P.; De Proft, F. *Phys. Chem. Chem. Phys.* **2014**, *16*, 14396–14407.
- (31) Alonso, M.; Geerlings, P.; De Proft, F. *Chem. Eur. J.* **2013**, *19*, 1617–1628.
- (32) Schreiner, P. R. *Angew. Chem., Int. Ed.* **2007**, *46*, 4217–4219.
- (33) Wodrich, M. D.; Corminboeuf, C.; Schleyer, P. v. R. *Org. Lett.* **2006**, *8*, 3631–3634.
- (34) Zhao, Y.; Truhlar, D. G. *Theor. Chem. Acc.* **2008**, *120*, 215–241.
- (35) Grimme, S. *J. Comput. Chem.* **2004**, *25*, 1463–1473.
- (36) Schleyer, P. v. R.; Maerker, C.; Dransfeld, A.; Jiao, H.; Hommes, N. J. R. v. E. *J. Am. Chem. Soc.* **1996**, *118*, 6317–6318.
- (37) AbuSalim, D. I.; Lash, T. D. *J. Org. Chem.* **2013**, *78*, 11535–11548.
- (38) AbuSalim, D. I.; Lash, T. D. *Org. Biomol. Chem.* **2013**, *11*, 8306–8323.
- (39) (a) Clezy, P. S.; Crowley, R. J.; Hai, T. T. *Aust. J. Chem.* **1982**, *35*, 411–421. (b) Jackson, A. H.; Kenner, G. W.; Smith, K. M.; Suckling, C. J. *J. Chem. Soc., Perkin Trans. 1* **1982**, 1441–1448. (c) Lash, T. D.; Lin, Y.; Novak, B. H.; Parikh, M. D. *Tetrahedron* **2005**, *61*, 11601–11614.
- (40) Frisch, M. J.; Trucks, G. W.; Schlegel, H. B.; Scuseria, G. E.; Robb, M. A.; Cheeseman, J. R.; Scalmani, G.; Barone, V.; Mennucci, B.; Petersson, G. A.; Nakatsuji, H.; Caricato, M.; Li, X.; Hratchian, H. P.; Izmaylov, A. F.; Bloino, J.; Zheng, G.; Sonnenberg, J. L.; Hada, M.; Ehara, M.; Toyota, K.; Fukuda, R.; Hasegawa, J.; Ishida, M.; Nakajima, T.; Honda, Y.; Kitao, O.; Nakai, H.; Vreven, T.; Montgomery, J. A., Jr.; Peralta, J. E.; Ogliaro, F.; Bearpark, M.; Heyd, J. J.; Brothers, E.; Kudin, K. N.; Staroverov, V. N.; Kobayashi, R.; Normand, J.; Raghavachari, K.; Rendell, A.; Burant, J. C.; Iyengar, S. S.; Tomasi, J.; Cossi, M.; Rega, N.; Millam, N. J.; Klene, M.; Knox, J. E.; Cross, J. B.; Bakken, V.; Adamo, C.; Jaramillo, J.; Gomperts, R.; Stratmann, R. E.; Yazyev, O.; Austin, A. J.; Cammi, R.; Pomelli, C.; Ochterski, J. W.; Martin, R. L.; Morokuma, K.; Zakrzewski, V. G.; Voth, G. A.; Salvador, P.; Dannenberg, J. J.; Dapprich, S.; Daniels, A. D.; Ö. Farkas, Foresman, J. B.; Ortiz, J. V.; Cioslowski, J.; Fox, D. J. *Gaussian 09, Revision D.01*; Gaussian, Inc., Wallingford, CT, 2009.
- (41) Wolinski, K.; Hinton, J. F.; Pulay, P. *J. Am. Chem. Soc.* **1990**, *112*, 8251–8260.